IJARCCE ISSN (O) 2278-1021, ISSN (P) 2319-5940

International Journal of Advanced Research in Computer and Communication Engineering

Impact Factor 8.471 ⁜ Peer-reviewed & Refereed journal ⁜ Vol. 14, Issue 5, May 2025

DOI: 10.17148/IJARCCE.2025.145122

# MODELLING AND ANALYSIS OF INDIAN RAILWAY WAGON WHEEL USING ANSYS AND ARTIFICIAL NEURAL NETWORK

**K. Suresh[1], G. L. N. Chaitanya[2], Dr. Y. Pratapa Reddy[3]**

U.G. Students, Department of Mechanical Engineering, KKR & KSR Institute of Technology and Sciences, Vinjanampadu, Vatticherukuru Mandal, Guntur District, AP, India[1,2]

Associate Professor, Department of Mechanical Engineering, KKR & KSR Institute of Technology and Sciences, Vinjanampadu, Vatticherukuru Mandal, Guntur District, AP, India [3]

**Abstract:** In the present study, the wear analysis of an Indian railway wagon wheel (IRWW) was modelled using modelling software CATIA and applied various material combinations and tested for its performance and wear slippage at distinct load applications. In the real-world applications, wear produces wheel-surface slippage, resulting in deformation and movement of the wheel beneath the track surface. To address this issue, a thorough investigation of rolling contact on train wheels was undertaken to lessen the likelihood of failure. In the present investigation, the IRWW was initially designed and modelled in CATIA and uploaded to ANSYS to make the analysis. The stress generated by increasing contact load at rail-wheel assembly in terms of stress, strain, total deformation, and safety factor were determined for various load applications. Later, the acquired results were validated using the Artificial Neural Network (ANN) of Machine Learning (ML) Approach. The results showed that the overall deformation applied under various loads was within the limit.

**Keywords:** CATIA, ANSYS, stress, strain, total deformation, IRWW, ANN

## I.INTRODUCTION

In 1825, the world's first train crossed the English countryside between Stockton and Darlington. R.M. Stephenson proposed the establishment of India's railway system (IRS) in 1844, and the East India Company (EIC) agreed. Various researchers executed distinct types of analysis using different modelling software like CATIA, SOLIDWORKS, ANSYS etc., with various loads. The wear phenomena should be focused on their impact on environmental costs and operational efficiency, with various experimental trials. A smartphone app uses convolutional neural networks to detect and classify railway wheel defects. Users take photographs of the wheels, which are evaluated by a trained convolutional neural networks **(**CNN) model. The app generates bar graphs for maintenance personnel, and reliability is assessed using metrics like accuracy, precision, recall, and F1 score **[1]**. The Anchor-Free Yolov8 (AFYv8) model, a deep learning-based classifier, has been proposed as a replacement for human wheel inspection in the Train Rolling Stock Examination (TRSE). Tests show that the model detects TRSEs with 10% higher accuracy than previous classifiers, potentially increasing railway safety and reducing operational disruptions **[2]**. Two machine learning methods are proposed to detect wheel defects in railway wagons, reducing noise and vibration emissions. The first uses distinct features to anticipate issues, while the second uses CNN **[3]**. Robotic systems are increasingly utilized in manufacturing to reduce costs, increase efficiency, and improve product and service. These automated machines, built with artificial intelligence and machine learning algorithms, are beneficial investments in automotive plants and hazardous environments like explosive disarming and radioisotope monitoring **[4]**. An enhanced YOLOv3 framework has been developed for rail wheel surface defect identification, achieving an average accuracy of 0.92, addressing the challenge of accurately classifying and positioning flaws **[5]**. A Deep Learning (DL) technique uses smartphone photos to identify tire tread flaws, enhancing automated predictive maintenance by reducing lead time and engineering hours, thereby ensuring railroad vehicle safety and rolling-stock asset lifespan **[6]**. The Indian Railway is developing a prototype railway coach to reduce maintenance costs and improve reliability, using event-driven maintenance approaches and ultrasonic vibration intensity to identify defects and prevent mishaps **[7]**. The study uses CAD models and FEA to analyse rail-wheel fatigue life under increasing axle loads and railway infrastructure growth, highlighting the importance of rail-wheel quality and physical contact **[8]**. The study explores the link between noise propagation, rail safety, and wheel wear on rolling stock, emphasizing the importance of detecting cracks early to prevent potential hazards **[9]**. The study examines the interface between railroad car wheels and rails, focusing on contact stresses from mechanical loads. It uses analytical and experimental techniques, including ANSYS's finite elements method, to evaluate wheel performance and wear estimation **[10]**.

IJARCCE ISSN (O) 2278-1021, ISSN (P) 2319-5940

International Journal of Advanced Research in Computer and Communication Engineering

Impact Factor 8.471 ⁜ Peer-reviewed & Refereed journal ⁜ Vol. 14, Issue 5, May 2025

DOI: 10.17148/IJARCCE.2025.145122

The project involves creating a 90-ton pay load trolley for cylindrical specimen transportation using propellants, using Ansys for structural analysis, Unigraphics for 3D modelling, and manual calculations **[11]**. Researchers and railroad businesses are using AutoCAD and Pro-E modelling programs, Universal Mechanism, and ANSYS to create virtual prototypes for predicting dynamic hopper wagon behaviour **[12]**. The study investigates the interaction between IRS-T12 rail wheels and UIC-60 using hand calculations and ANSYS. It compares manually estimated stresses and a three-dimensional finite element model, comparing results with hand calculations. Further analysis is recommended **[13]**. The study uses ANSYS and a three-dimensional finite element study to analyse the impact of axle load and train speed on rail junction performance, suggesting modifications to rail design **[14]**. The study investigated the impact of wheel re-profiling on deformations and stresses resulting from mechanical and thermal loads on a rail loco wheel using ANSYS software **[15]**.

## II. MATERIALS

### 2.1 Chemical compositions and Specifications

In the present work, the list of materials mentioned in Table-1 are considered for analysis in ANSYS after the IRWW was designed and modelled in CATIA. The nominal chemical composition of various materials and their specifications are summarized for the listed materials in the next Tables.

Table-1: List of various materials used for analysis in ANSYS

| MATERIAL NUMBER | MATERIAL NAME | FEATURES |
|---|---|---|
| M-I | HIGH CARBON STEEL-1095 | Hardened and tempered |
| M-II | HIGH CARBON STEEL-1340 | Hardened and tempered |
| M-III | LOW ALLOY STEEL-4135 | Hardened and tempered |
| M-IV | ALLOY STEEL, TRIP, **YS450** | ----- |

### 2.2 MATERIAL - I: (HIGH CARBON STEEL – 1095)

HCS-1095 steel, a high-carbon steel, is heat-treated by hardening (heating and quenching) and tempering to obtain hardness and toughness, making it ideal for applications that require sharp edges and edge retention. The Chemical composition and specifications of material-II (HCS-1095) are listed in Table-2 and Table-3.

Table 2*:* **Chemical** Composition of Material-I (HCS- 1095 hardened & tempered) in wt.%

| Elements | Carbon | Manganese | Silicon | Phosphorus | Sulphur | Iron |
|---|---|---|---|---|---|---|
| **Acronym** | **C** | **Mn** | **Si** | **P** | **S** | **Fe** |
| **HCS- 1095 Hardened and Tempered** | 0.90-1.03 | 0.30-0.50 | 0.15-0.35 | Max 0.040 | Max 0.050 | 0.25 |

HCS-1095 steel is plain carbon steel, meaning it primarily relies on carbon for its strength and hardenability, with manganese and silicon present in small amounts.

Table 3: Specifications of Material-I (HCS-1095 Hardened & tempered)

| Material | Youngs Modulus (MPa) | Poisson's ratio | Bulk Modulus (MPa) | Shear Modulus (MPa) | Tensile Yield Strength (MPa) | Tensile Ultimate Strength (MPa) | Density (Kg/m3) | Coefficient of Thermal Expansion (/ $^0$C) |
|---|---|---|---|---|---|---|---|---|
| **HCS-1095 (Hardened & tempered)** | 221800 | 0.29 | 176030 | 85969 | 1042 | 1480 | 7850 | 0.000007457 |

### 2.3 MATERIAL -II (HIGH CARBON STEEL-1340)

HCS-1340 steel is a carbon-manganese alloy that can be hardened and tempered. The Chemical composition and specifications of material-II (HCS-1340) are listed in Table-4 and Table-5. It normally includes 0.38-0.43% carbon and 1.60 -1.90% manganese.

IJARCCE ISSN (O) 2278-1021, ISSN (P) 2319-5940

International Journal of Advanced Research in Computer and Communication Engineering

Impact Factor 8.471 ⁜ Peer-reviewed & Refereed journal ⁜ Vol. 14, Issue 5, May 2025

DOI: 10.17148/IJARCCE.2025.145122

Table 4: **Chemical Composition** of Material-II (HCS- 1340 hardened & tempered)

| Elements | Carbon | Manganese | Silicon | Iron |
|---|---|---|---|---|
| **Acronym** | **C** | **Mn** | **Si** | **Fe** |
| **HCS- 1340 Hardened and Tempered** | 0.38-0.43 % | 1.60-1.90 % | 0.15-0.35 % | remaining % |

Table 5: **Specifications** of Material-II (HCS-1340 Hardened & tempered)

| Material | Youngs Modulus (MPa) | Poisson's ratio | Bulk Modulus (MPa) | Shear Modulus (MPa) | Tensile Yield Strength (MPa) | Tensile Ultimate Strength (MPa) | Density ($Kg/m^3$) | Coefficient of Thermal Expansion ($/^0C$) |
|---|---|---|---|---|---|---|---|---|
| **HCS-1340 (Hardened & tempered)** | 207400 | 0.29 | 164600 | 80388 | 1584 | 1798 | 7850 | 0.00001195 |

### 2.4 MATERIAL -III (LOW ALLOY STEEL-4135)

LAS-AISI 4135 steel is well-known for its high strength-to-weight ratio and improved qualities brought about by heat treatment, particularly hardening and tempering, which makes it appropriate for a range of applications needing strong material performance. The Chemical composition and specifications of MATERIAL-III (**Low Alloy Steel-4135**) are listed in Table-6 and Table-7.

Table 6*:* **Chemical** Composition of Material-III (Low Alloy 4135 Steel Hardened and Tempered)

| Acronym | C | Mn | Si | P | Cr | Fe | Mo |
|---|---|---|---|---|---|---|---|
| **Low Alloy Steel - 4135 Hardened and Tempered** | 0.33-0.38 | 0.70-0.90 | 0.15-0.35 | ≤ 0.035 | 0.80-1.10 | 97-98 | 0.15-0.25 |

Table 7: **Specifications** of Material-III (Low Alloy Steel- 4135, Hardened and Tempered)

| Material | Youngs Modulus (MPa) | Poisson's ratio | Bulk Modulus (MPa) | Shear Modulus (MPa) | Tensile Yield Strength (MPa) | Tensile Ultimate Strength (MPa) | Density (Kg/m3) | Coefficient of Thermal Expansion ($/ ^0C$) |
|---|---|---|---|---|---|---|---|---|
| **Low Alloy Steel-4135 (Hardened and Tempered)** | 221060 | 0.3265 | 203100 | 79382 | 915.2 | 1090 | 7850 | 0.00001273 |

### 2.5 MATERIAL -IV (ALLOY STEEL, TRIP, YS450)

YS450-steel alloyed with vanadium, molybdenum, and chromium. Aircraft and missile components are among the uses for it that call for great strength, durability, and resistance to heat and wear. The Chemical composition and specifications of MATERIAL-IV (**Alloy steel, TRIP, YS450**) are listed in Table-8 and Table-9.

Table 8: **Chem**ical Composition of Material-IV (Alloy steel, TRIP, YS450)

| Elements | Carbon | Manganese | Silicon | Phosphorus | Aluminum | Chromium | Sulphur | Nickel | Molybdenum |
|---|---|---|---|---|---|---|---|---|---|
| **Acronym** | **C** | **Mn** | **Si** | **P** | **Al** | **Cr** | **S** | **Ni** | **Mo** |
| **Alloy steel, TRIP, YS450** | 0.10-0.25 | 1.5-2.5 | 0.5-1.5 | ≤ 0.03 | 0.01-0.10 | 0.1-0.5 | ≤ 0.01 | 0-0.5 | 0 - 0.15 |

Table 9*:* **Specifications** of Material-IV (Alloy steel, TRIP, YS450)

| Material | Youngs Modulus (MPa) | Poisson's ratio | Bulk Modulus (MPa) | Shear Modulus (MPa) | Tensile Yield Strength (MPa) | Tensile Ultimate Strength (MPa) | Density (Kg/m3) | Coefficient of Thermal Expansion ($C^{-1}$) |
|---|---|---|---|---|---|---|---|---|
| **Alloy steel, TRIP, YS450** | 221800 | 0.3 | 184800 | 85308 | 519.6 | 837.9 | 7850 | 0.00001196 |

IJARCCE ISSN (O) 2278-1021, ISSN (P) 2319-5940

International Journal of Advanced Research in Computer and Communication Engineering

Impact Factor 8.471 ⁜ Peer-reviewed & Refereed journal ⁜ Vol. 14, Issue 5, May 2025

DOI: 10.17148/IJARCCE.2025.145122

## III. DESIGN OF WHEEL IN CATIA

The internal components of the IRWW are shown in Figure 3.1, and its modelling in shown in Figure 3.1(a) to Figure 3.2 (h). In general, the actual railway wagon wheel is made without any slots in it, in the present design a hexagonal slot is introduced to check its performance and reduction of weight and save the material while fabrication.

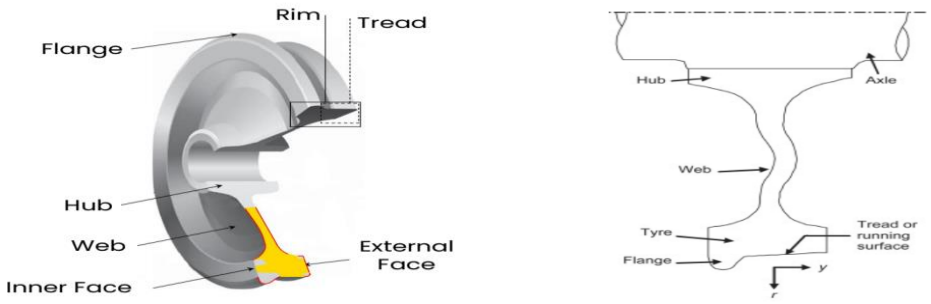


Figure 3.1: Nomenclature of IRWW

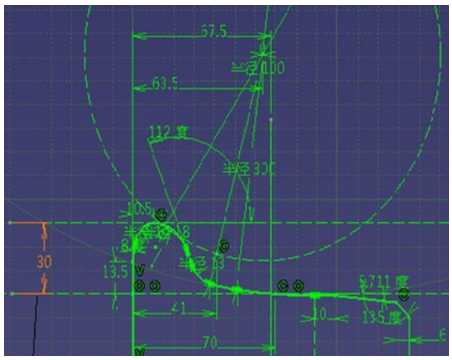

(a) 2D illustration of the IRWW

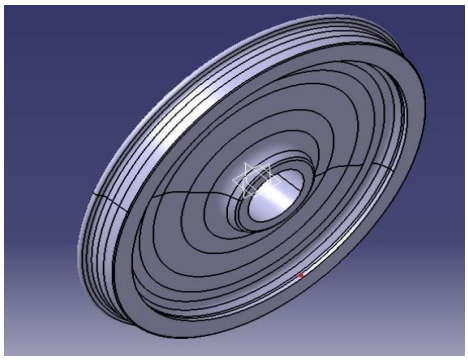

(b) External Part of the IRWW

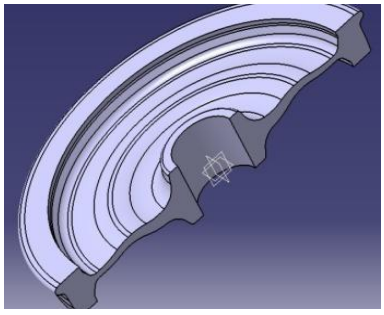

(c) Sectional Analysis of the IRWW.

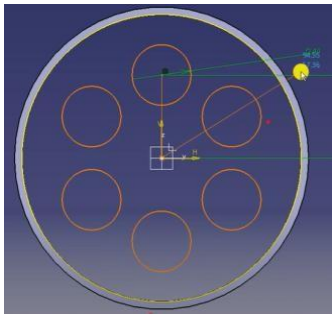

(d) Slot creation in 2D sketch.

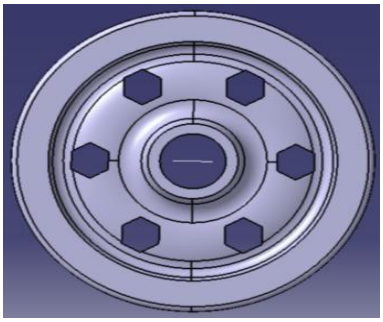

(e) Reduction of material through design

(f)

IJARCCE ISSN (O) 2278-1021, ISSN (P) 2319-5940

International Journal of Advanced Research in Computer and Communication Engineering

Impact Factor 8.471 ⁜ Peer-reviewed & Refereed journal ⁜ Vol. 14, Issue 5, May 2025

DOI: 10.17148/IJARCCE.2025.145122

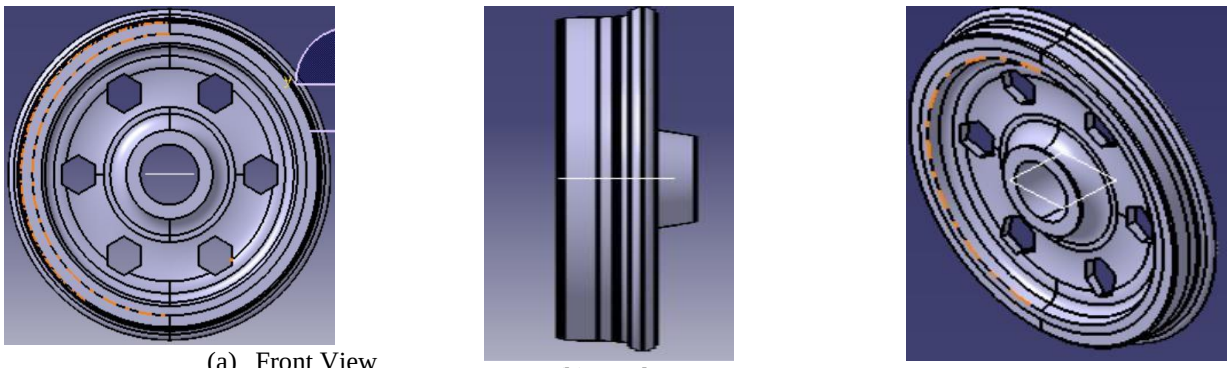

(a) Front View (b) Side view (c) Isometric View

Figure 3.2: Modelling of Railway wagon wheel with Array of slot

## IV. FINITE ELEMENT ANALYSIS OF WHEEL USING ANSYS

ANSYS, developed by John Swanson in 1970, is a finite element analysis (FEA) software that saves time and money in product evaluation, ensuring precise and effective product development. ANSYS helps engineers understand how their products work under real-world conditions, using numerical approaches for civil structure and mechanical product design.

### 4.1 BOUNDARY CONDITIONS

Material properties like Density, Youngs Modulus, Tensile Yield Strength and other details are shown in Figure-4.1.
In the present analysis the meshing is done by selecting the Tetrahedra element with 5 mm size of the element. The meshing details like mesh quality, element size, number of nodes and other details are shown in Figure-4.2.
The contact details between rail and wheel are described in Figure-4.3. The Force and Displacement details are described in Figure -4.4 and Figure-4.5.

Details of "Carbon steel, 1340, hardened & temp

| | |
|---|---|
| **Common Material Properties** | |
| Density | 7850 kg/m³ |
| Young's Modulus | 2.074e+11 Pa |
| Thermal Conductivity | 49.75 W/m·°C |
| Specific Heat | 478.3 J/kg·°C |
| Tensile Yield Strength | 1.584e+09 Pa |
| Tensile Ultimate Strength | 1.798e+09 Pa |
| Nonlinear Behavior | True |
| Full Details | Click To View Full Details |
| **Statistics** | |
| Assigned Bodies | 2 |

Figure 4.1: Properties of Materials

tails of "Mesh"

| | |
|---|---|
| **Display** | |
| Display Style | Use Geometry Set |
| **Defaults** | |
| Physics Preference | Mechanical |
| Element Order | Program Controll |
| Element Size | 5.0 mm |
| **Sizing** | |
| Use Adaptive Sizing | Yes |
| Resolution | 7 |
| Mesh Defeaturing | Yes |
| Defeature Size | Default |
| Transition | Fast |
| Span Angle Center | Fine |
| Initial Size Seed | Assembly |
| Bounding Box Diagonal | 1992.8 mm |
| Average Surface Area | 41661 mm² |
| Minimum Edge Length | 2.3362e-003 mm |

| | |
|---|---|
| **Quality** | |
| Check Mesh Quality | Yes, Errors |
| Error Limits | Aggressive Mechar |
| Target Element Qual... | Default (5.e-002) |
| Smoothing | Medium |
| Mesh Metric | None |
| **Inflation** | |
| **Advanced** | |
| Number of CPUs for Pa... | Program Controlle |
| Straight Sided Elements | No |
| Rigid Body Behavior | Dimensionally Red |
| Triangle Surface Mesher | Program Controlle |
| Topology Checking | Yes |
| Pinch Tolerance | Please Define |
| Generate Pinch on Refr... | No |
| **Statistics** | |
| Nodes | 1696489 |
| Elements | 1062406 |


Figure 4.2: Meshing of Wheel

IJARCCE ISSN (O) 2278-1021, ISSN (P) 2319-5940

International Journal of Advanced Research in Computer and Communication Engineering

Impact Factor 8.471 ⁜ Peer-reviewed & Refereed journal ⁜ Vol. 14, Issue 5, May 2025

DOI: 10.17148/IJARCCE.2025.145122

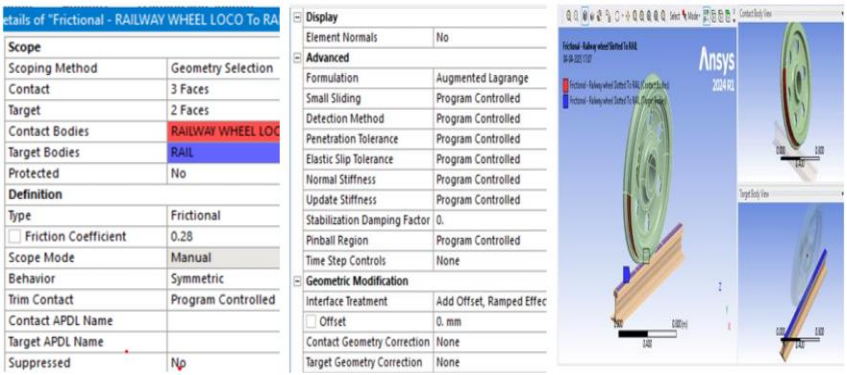

| etails of "Frictional - RAILWAY WHEEL LOCO To RA | |
|---|---|
| **Scope** | |
| Scoping Method | Geometry Selection |
| Contact | 3 Faces |
| Target | 2 Faces |
| Contact Bodies | RAILWAY WHEEL LOC |
| Target Bodies | RAIL |
| Protected | No |
| **Definition** | |
| Type | Frictional |
| Friction Coefficient | 0.28 |
| Scope Mode | Manual |
| Behavior | Symmetric |
| Trim Contact | Program Controlled |
| Contact APDL Name | |
| Target APDL Name | |
| Suppressed | No |

| Display | |
|---|---|
| Element Normals | No |
| **Advanced** | |
| Formulation | Augmented Lagrange |
| Small Sliding | Program Controlled |
| Detection Method | Program Controlled |
| Penetration Tolerance | Program Controlled |
| Elastic Slip Tolerance | Program Controlled |
| Normal Stiffness | Program Controlled |
| Update Stiffness | Program Controlled |
| Stabilization Damping Factor | 0. |
| Pinball Region | Program Controlled |
| Time Step Controls | None |
| **Geometric Modification** | |
| Interface Treatment | Add Offset, Ramped Effec |
| Offset | 0. mm |
| Contact Geometry Correction | None |
| Target Geometry Correction | None |

Figure 4.3: Details of contact information between two bodies

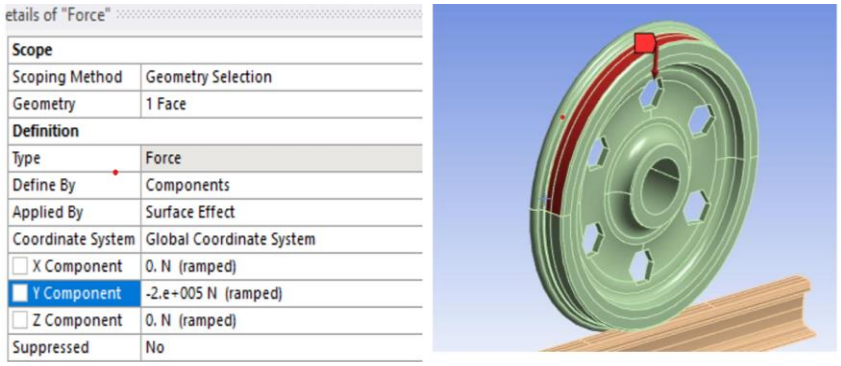

| etails of "Force" | |
|---|---|
| **Scope** | |
| Scoping Method | Geometry Selection |
| Geometry | 1 Face |
| **Definition** | |
| Type | Force |
| Define By | Components |
| Applied By | Surface Effect |
| Coordinate System | Global Coordinate System |
| X Component | 0. N (ramped) |
| Y Component | -2.e+005 N (ramped) |
| Z Component | 0. N (ramped) |
| Suppressed | No |

Figure 4.4: Details of Force application

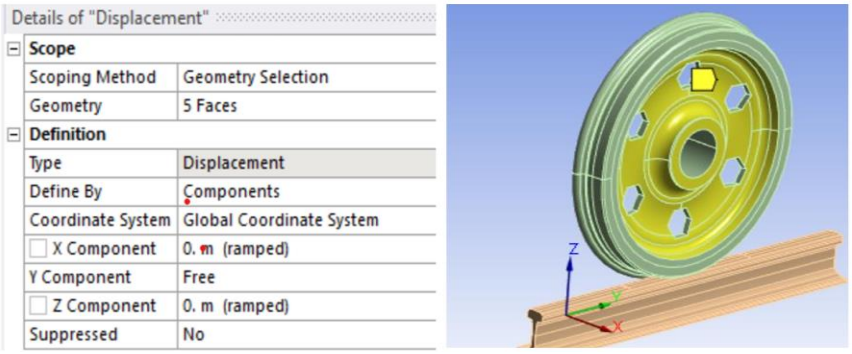

| Details of "Displacement" | |
|---|---|
| **Scope** | |
| Scoping Method | Geometry Selection |
| Geometry | 5 Faces |
| **Definition** | |
| Type | Displacement |
| Define By | Components |
| Coordinate System | Global Coordinate System |
| X Component | 0. m (ramped) |
| Y Component | Free |
| Z Component | 0. m (ramped) |
| Suppressed | No |

Figure 4.5: Details of Displacement

## V. MACHINE LEARNING

Machine Learning (ML) has been defined in a variety of formal ways. Alpaydin (2016) described machine learning as "using example data or prior experience to program computers to optimize a performance criterion." Burkov (2019) stated ML as "a branch of computer science that allows computer programs to conduct planning, diagnosis, prediction, and behaviour pattern recognition by learning from historical data, i.e., without prior knowledge."

### 5.1 ARTIFIICAL NEURAL NETWORK (ANN)

An artificial neural network (ANN) is a computational model that processes input data through layers of interconnected neurons or nodes to predict output. It can execute classification and regression tasks, with one task common for each network.

ANNs can be classified as supervised or unsupervised based on their learning type. They learn basic principles from symbolic situations rather than human-established laws. ANNs are widely used in various industries due to their ability to learn from examples, making them beneficial for systems with large amounts of complex and ambiguous information. The layers consist of an input, hidden, and output layer.

IJARCCE ISSN (O) 2278-1021, ISSN (P) 2319-5940

International Journal of Advanced Research in Computer and Communication Engineering

Impact Factor 8.471 ⁜ Peer-reviewed & Refereed journal ⁜ Vol. 14, Issue 5, May 2025

DOI: 10.17148/IJARCCE.2025.145122

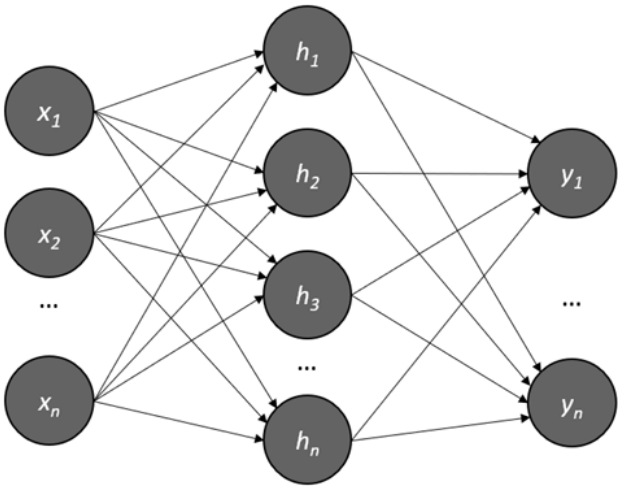


Figure 5.1: Diagram of Artificial Neural Network

## VI. METHODOLOGY

The flow chart of the modelling and analysis of the present work is described in Figure 6.1, where the work is carried out in three stages.

In Stage-I, the modelling and design of the railway wagon wheel was done using the modelling CATIA software,

Later in Stage-II, the outcomes from the CATIA were uploaded to ANSYS and the analysis part of the wagon wheel has been caried out at various load applications with different materials.

Further, in Stage-III of the work, the obtained results from the ANSYS analysis at different loads for different materials are summarised and taken as input data and are submitted to the ANN module of MATLAB, to analyse the outcomes, by training, testing and validating the ANSYS results with the help of neural network.


Figure 6.1: Flowchart of methodology of work

IJARCCE ISSN (O) 2278-1021, ISSN (P) 2319-5940

International Journal of Advanced Research in Computer and Communication Engineering

Impact Factor 8.471 ⁜ Peer-reviewed & Refereed journal ⁜ Vol. 14, Issue 5, May 2025

DOI: 10.17148/IJARCCE.2025.145122

## VII. RESULTS AND DISCUSSIONS

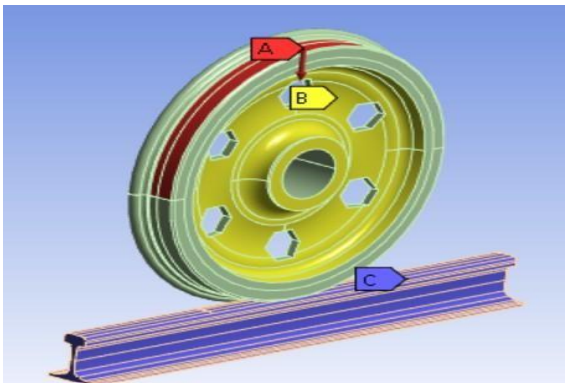


Figure 7.1: Load Application of 90000N

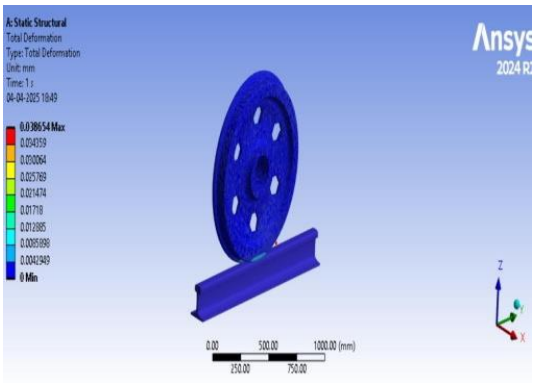


Figure 7.2: Total Deformation (at 90000N)

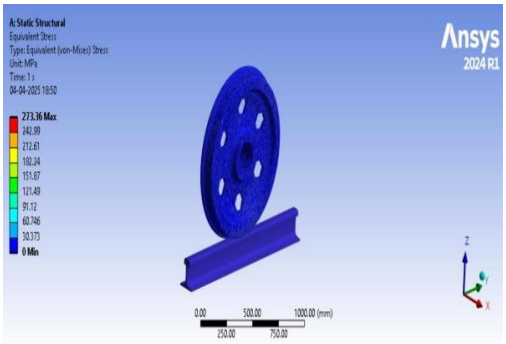


Figure 7.3: Equivalent (von-mises) Stress (at 90000N)

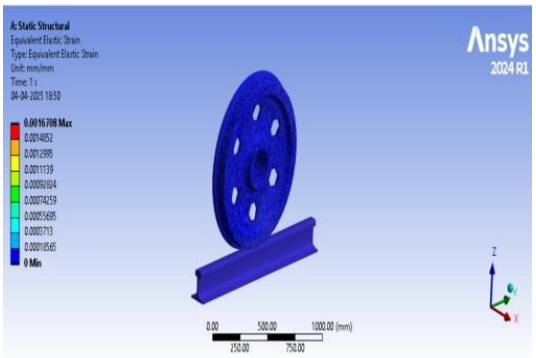


Figure 7.4: Equivalent Elastic Strain (at 90000N)

Table 7.1: Total deformation of Materials at various loads

| Load (KN) | HCS- 1095 (Hardened & Tempered) | HCS-1340 (Hardened & Tempered) | Alloy steel, TRIP YS 450 | LOW ALLOY STEEL 4135 (Hardened & Tempered) |
|---|---|---|---|---|
| 90 | 0.08665 | 0.085252 | 0.08309 | 0.0852226 |
| 180 | 0.12176 | 0.12323 | 0.1202 | 0.1232000 |
| 270 | 0.15353 | 0.15707 | 0.13729 | 0.1569700 |
| 360 | 0.18445 | 0.1885 | 0.18356 | 0.1882300 |
| 450 | 0.21232 | 0.21827 | 0.21237 | 0.2177400 |
| 540 | 0.23893 | 0.24627 | 0.23953 | 0.2454600 |
| 630 | 0.26425 | 0.2728 | 0.26513 | 0.2716500 |

IJARCCE ISSN (O) 2278-1021, ISSN (P) 2319-5940

International Journal of Advanced Research in Computer and Communication Engineering

Impact Factor 8.471 ⁜ Peer-reviewed & Refereed journal ⁜ Vol. 14, Issue 5, May 2025

DOI: 10.17148/IJARCCE.2025.145122

### 7.1 ANN RESULTS

| INPUTS | | | | | | | | | |
|---|---|---|---|---|---|---|---|---|---|
| FORCE ANALYSIS | | | | | | | | | |
| | Youngs | Poisson's | Bulk | Shear | Tensile Yield | Tensile Ultimate | Density (Kg/m3) | Coefficient of Thermal Expansion | Load(KN) |
| HCS-1095 | 221800 | 0.29 | 176030 | 85969 | 1042 | 1480 | 7850 | 0.000007457 | 90 |
| | 221800 | 0.29 | 176030 | 85969 | 1042 | 1480 | 7850 | 0.000007457 | 180 |
| | 221800 | 0.29 | 176030 | 85969 | 1042 | 1480 | 7850 | 0.000007457 | 270 |
| | 221800 | 0.29 | 176030 | 85969 | 1042 | 1480 | 7850 | 0.000007457 | 360 |
| | 221800 | 0.29 | 176030 | 85969 | 1042 | 1480 | 7850 | 0.000007457 | 450 |
| | 221800 | 0.29 | 176030 | 85969 | 1042 | 1480 | 7850 | 0.000007457 | 540 |
| | 221800 | 0.29 | 176030 | 85969 | 1042 | 1480 | 7850 | 0.000007457 | 630 |
| HCS-1340 | 207400 | 0.29 | 164600 | 80388 | 1584 | 1798 | 7850 | 0.00001195 | 90 |
| | 207400 | 0.29 | 164600 | 80388 | 1584 | 1798 | 7850 | 0.00001195 | 180 |
| | 207400 | 0.29 | 164600 | 80388 | 1584 | 1798 | 7850 | 0.00001195 | 270 |
| | 207400 | 0.29 | 164600 | 80388 | 1584 | 1798 | 7850 | 0.00001195 | 360 |
| | 207400 | 0.29 | 164600 | 80388 | 1584 | 1798 | 7850 | 0.00001195 | 450 |
| | 207400 | 0.29 | 164600 | 80388 | 1584 | 1798 | 7850 | 0.00001195 | 540 |
| | 207400 | 0.29 | 164600 | 80388 | 1584 | 1798 | 7850 | 0.00001195 | 630 |
| LA-4135 | 221060 | 0.3265 | 203100 | 79382 | 915.2 | 1090 | 7850 | 0.00001273 | 90 |
| | 221060 | 0.3265 | 203100 | 79382 | 915.2 | 1090 | 7850 | 0.00001273 | 180 |
| | 221060 | 0.3265 | 203100 | 79382 | 915.2 | 1090 | 7850 | 0.00001273 | 270 |
| | 221060 | 0.3265 | 203100 | 79382 | 915.2 | 1090 | 7850 | 0.00001273 | 360 |
| | 221060 | 0.3265 | 203100 | 79382 | 915.2 | 1090 | 7850 | 0.00001273 | 450 |
| | 221060 | 0.3265 | 203100 | 79382 | 915.2 | 1090 | 7850 | 0.00001273 | 540 |
| | 221060 | 0.3265 | 203100 | 79382 | 915.2 | 1090 | 7850 | 0.00001273 | 630 |
| Alloy trip | 221800 | 0.3 | 184800 | 85308 | 519.6 | 837.9 | 7850 | 0.00001196 | 90 |
| | 221800 | 0.3 | 184800 | 85308 | 519.6 | 837.9 | 7850 | 0.00001196 | 180 |
| | 221800 | 0.3 | 184800 | 85308 | 519.6 | 837.9 | 7850 | 0.00001196 | 270 |
| | 221800 | 0.3 | 184800 | 85308 | 519.6 | 837.9 | 7850 | 0.00001196 | 360 |
| | 221800 | 0.3 | 184800 | 85308 | 519.6 | 837.9 | 7850 | 0.00001196 | 450 |
| | 221800 | 0.3 | 184800 | 85308 | 519.6 | 837.9 | 7850 | 0.00001196 | 540 |
| | 221800 | 0.3 | 184800 | 85308 | 519.6 | 837.9 | 7850 | 0.00001196 | 630 |

Figure 7.5: Input Data-I

| INPUTS | | | | | | | | | |
|---|---|---|---|---|---|---|---|---|---|
| ROTATIONAL VELOCITY ANALYSIS | | | | | | | | | |
| | Youngs | Poisson's | Bulk | Shear | Tensile Yield | Tensile Ultimate | Density (Kg/m3) | Coefficient of Thermal Expansion | Load(KN) |
| HCS-1095 | 221800 | 0.29 | 176030 | 85969 | 1042 | 1480 | 7850 | 0.000007457 | 70 |
| | 221800 | 0.29 | 176030 | 85969 | 1042 | 1480 | 7850 | 0.000007457 | 120 |
| | 221800 | 0.29 | 176030 | 85969 | 1042 | 1480 | 7850 | 0.000007457 | 170 |
| | 221800 | 0.29 | 176030 | 85969 | 1042 | 1480 | 7850 | 0.000007457 | 220 |
| | 221800 | 0.29 | 176030 | 85969 | 1042 | 1480 | 7850 | 0.000007457 | 270 |
| | 221800 | 0.29 | 176030 | 85969 | 1042 | 1480 | 7850 | 0.000007457 | 320 |
| | 221800 | 0.29 | 176030 | 85969 | 1042 | 1480 | 7850 | 0.000007457 | 370 |
| HCS-1340 | 207400 | 0.29 | 164600 | 80388 | 1584 | 1798 | 7850 | 0.00001195 | 70 |
| | 207400 | 0.29 | 164600 | 80388 | 1584 | 1798 | 7850 | 0.00001195 | 120 |
| | 207400 | 0.29 | 164600 | 80388 | 1584 | 1798 | 7850 | 0.00001195 | 170 |
| | 207400 | 0.29 | 164600 | 80388 | 1584 | 1798 | 7850 | 0.00001195 | 220 |
| | 207400 | 0.29 | 164600 | 80388 | 1584 | 1798 | 7850 | 0.00001195 | 270 |
| | 207400 | 0.29 | 164600 | 80388 | 1584 | 1798 | 7850 | 0.00001195 | 320 |
| | 207400 | 0.29 | 164600 | 80388 | 1584 | 1798 | 7850 | 0.00001195 | 370 |
| LA-4135 | 221060 | 0.3265 | 203100 | 79382 | 915.2 | 1090 | 7850 | 0.00001273 | 70 |
| | 221060 | 0.3265 | 203100 | 79382 | 915.2 | 1090 | 7850 | 0.00001273 | 120 |
| | 221060 | 0.3265 | 203100 | 79382 | 915.2 | 1090 | 7850 | 0.00001273 | 170 |
| | 221060 | 0.3265 | 203100 | 79382 | 915.2 | 1090 | 7850 | 0.00001273 | 220 |
| | 221060 | 0.3265 | 203100 | 79382 | 915.2 | 1090 | 7850 | 0.00001273 | 270 |
| | 221060 | 0.3265 | 203100 | 79382 | 915.2 | 1090 | 7850 | 0.00001273 | 320 |
| | 221060 | 0.3265 | 203100 | 79382 | 915.2 | 1090 | 7850 | 0.00001273 | 370 |
| Alloy trip | 221800 | 0.3 | 184800 | 85308 | 519.6 | 837.9 | 7850 | 0.00001196 | 70 |
| | 221800 | 0.3 | 184800 | 85308 | 519.6 | 837.9 | 7850 | 0.00001196 | 120 |
| | 221800 | 0.3 | 184800 | 85308 | 519.6 | 837.9 | 7850 | 0.00001196 | 170 |
| | 221800 | 0.3 | 184800 | 85308 | 519.6 | 837.9 | 7850 | 0.00001196 | 220 |
| | 221800 | 0.3 | 184800 | 85308 | 519.6 | 837.9 | 7850 | 0.00001196 | 270 |
| | 221800 | 0.3 | 184800 | 85308 | 519.6 | 837.9 | 7850 | 0.00001196 | 320 |
| | 221800 | 0.3 | 184800 | 85308 | 519.6 | 837.9 | 7850 | 0.00001196 | 370 |

Figure 7.6: Input Data-II

IJARCCE ISSN (O) 2278-1021, ISSN (P) 2319-5940

International Journal of Advanced Research in Computer and Communication Engineering

Impact Factor 8.471 ⁜ Peer-reviewed & Refereed journal ⁜ Vol. 14, Issue 5, May 2025

DOI: 10.17148/IJARCCE.2025.145122

| OUTPUTS | | | |
|---|---|---|---|
| FORCE ANALYSIS | | | |
| | TOTAL DEFORMATION | Equivalent Strain | Equivalent Stress |
| HCS-1095 | 0.08665 | 0.0045261 | 890.78 |
| | 0.12176 | 0.0049687 | 976.25 |
| | 0.15353 | 0.0052236 | 1060.6 |
| | 0.18445 | 0.0054531 | 1108.2 |
| | 0.21232 | 0.0054388 | 1111.3 |
| | 0.23893 | 0.0053342 | 1082.2 |
| | 0.26425 | 0.005387 | 1112.7 |
| HCS-1340 | 0.085252 | 0.0043105 | 861.57 |
| | 0.12323 | 0.0050047 | 1004.6 |
| | 0.15707 | 0.0053383 | 1075.5 |
| | 0.1885 | 0.0053539 | 1102.8 |
| | 0.21827 | 0.005333 | 1107.7 |
| | 0.24627 | 0.0054001 | 1115.3 |
| | 0.2728 | 0.0053767 | 1116.1 |
| LOW ALLOY STEEL 4135 | 0.0852226 | 0.00043095 | 861.65 |
| | 0.1232000 | 0.0055025 | 1116.5 |
| | 0.1569700 | 0.0064631 | 1325.2 |
| | 0.1882300 | 0.0072311 | 1493.5 |
| | 0.2177400 | 0.0075912 | 1563.8 |
| | 0.2454600 | 0.0076839 | 1587.7 |
| | 0.2716500 | 0.0078434 | 1622.6 |
| Alloy Trip YS 450 | 0.08309 | 0.0041369 | 830.22 |
| | 0.1202 | 0.0052991 | 1078.6 |
| | 0.13729 | 0.0062369 | 1282.2 |
| | 0.18356 | 0.0070587 | 1461.1 |
| | 0.21237 | 0.007705 | 1603.1 |
| | 0.23953 | 0.0082242 | 1717.4 |
| | 0.26513 | 0.0083635 | 1741.1 |

Figure 7.7: Output Data-I

| OUTPUTS | | | |
|---|---|---|---|
| `ROTATIONAL VELOCITY ANALYSIS | | | |
| | TOTAL DEFORMATION | Equivalent Strain | Equivalent Stress |
| HCS-1095 | 0.027378 | 0.00012606 | 24.817 |
| | 0.080458 | 0.00037045 | 72.931 |
| | 0.16147 | 0.00074347 | 146.37 |
| | 0.27043 | 0.0012451 | 245.13 |
| | 0.40732 | 0.0018754 | 369.21 |
| | 0.57214 | 0.0026343 | 518.62 |
| | 0.76491 | 0.0035218 | 693.35 |
| HCS-1340 | 0.028041 | 0.00012911 | 24.817 |
| | 0.0820405 | 0.00037942 | 72.931 |
| | 0.16538 | 0.00076147 | 146.37 |
| | 0.27697 | 0.0012753 | 245.13 |
| | 0.41718 | 0.0019208 | 369.21 |
| | 0.58599 | 0.0026981 | 518.62 |
| | 0.78342 | 0.0036071 | 693.35 |
| LOW ALLOY STEEL 4135 | 0.02838 | 0.0001321 | 25.138 |
| | 0.083403 | 0.00038822 | 73.875 |
| | 0.16739 | 0.00077914 | 148.26 |
| | 0.28033 | 0.0013049 | 2483.3 |
| | 0.42223 | 0.0019654 | 373.99 |
| | 0.59309 | 0.0027607 | 525.33 |
| | 0.69309 | 0.0027607 | 625.33 |
| Alloy Trip YS 450 | 0.02742 | 0.0001266 | 24.92 |
| | 0.08058 | 0.00037208 | 73.235 |
| | 0.16172 | 0.00074674 | 146.98 |
| | 0.27084 | 0.0012506 | 246.15 |
| | 0.40794 | 0.0018836 | 370.75 |
| | 0.57301 | 0.0026459 | 506.8 |
| | 0.76605 | 0.0027145 | 532.03 |

Figure 7.8: Output Data-II

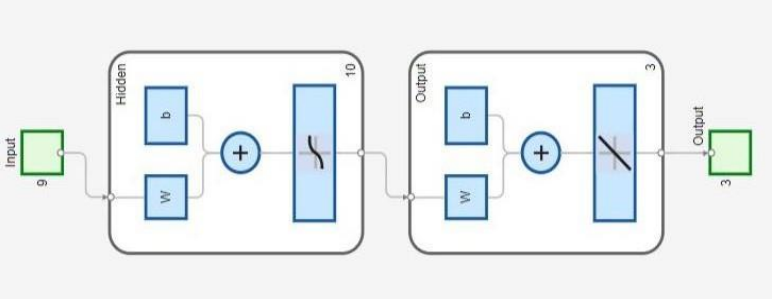


Figure 7.9: Neural Network for the given input and output in ANN

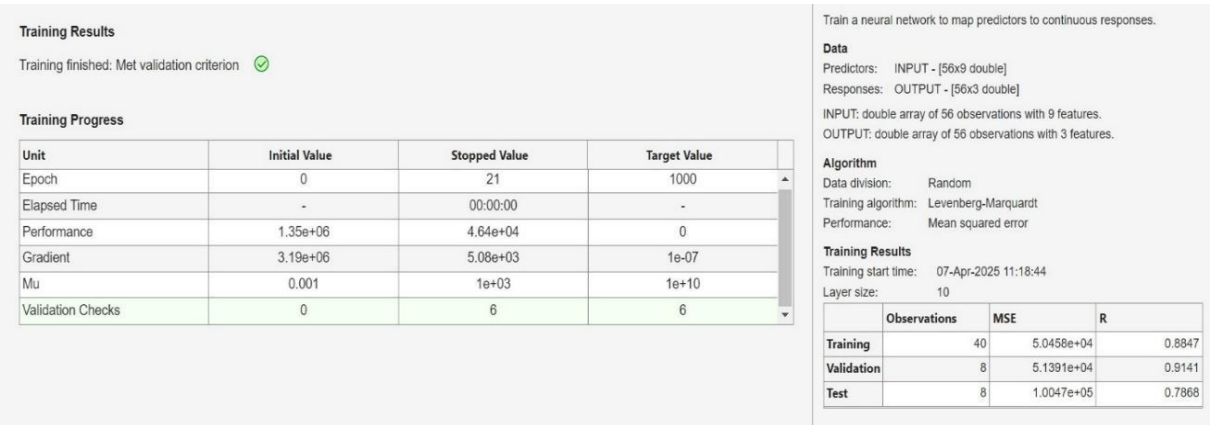

**Training Results**

Training finished: Met validation criterion

**Training Progress**

| Unit | Initial Value | Stopped Value | Target Value |
|---|---|---|---|
| Epoch | 0 | 21 | 1000 |
| Elapsed Time | - | 00:00:00 | - |
| Performance | 1.35e+06 | 4.64e+04 | 0 |
| Gradient | 3.19e+06 | 5.08e+03 | 1e-07 |
| Mu | 0.001 | 1e+03 | 1e+10 |
| Validation Checks | 0 | 6 | 6 |

Train a neural network to map predictors to continuous responses.

**Data**

Predictors: INPUT - [56x9 double]

Responses: OUTPUT - [56x3 double]

INPUT: double array of 56 observations with 9 features.

OUTPUT: double array of 56 observations with 3 features.

**Algorithm**

Data division: Random

Training algorithm: Levenberg-Marquardt

Performance: Mean squared error

**Training Results**

Training start time: 07-Apr-2025 11:18:44

Layer size: 10

| | Observations | MSE | R |
|---|---|---|---|
| Training | 40 | 5.0458e+04 | 0.8847 |
| Validation | 8 | 5.1391e+04 | 0.9141 |
| Test | 8 | 1.0047e+05 | 0.7868 |

Figure 7.10: Details of Training

IJARCCE ISSN (O) 2278-1021, ISSN (P) 2319-5940

International Journal of Advanced Research in Computer and Communication Engineering

Impact Factor 8.471 ⁜ Peer-reviewed & Refereed journal ⁜ Vol. 14, Issue 5, May 2025

DOI: 10.17148/IJARCCE.2025.145122

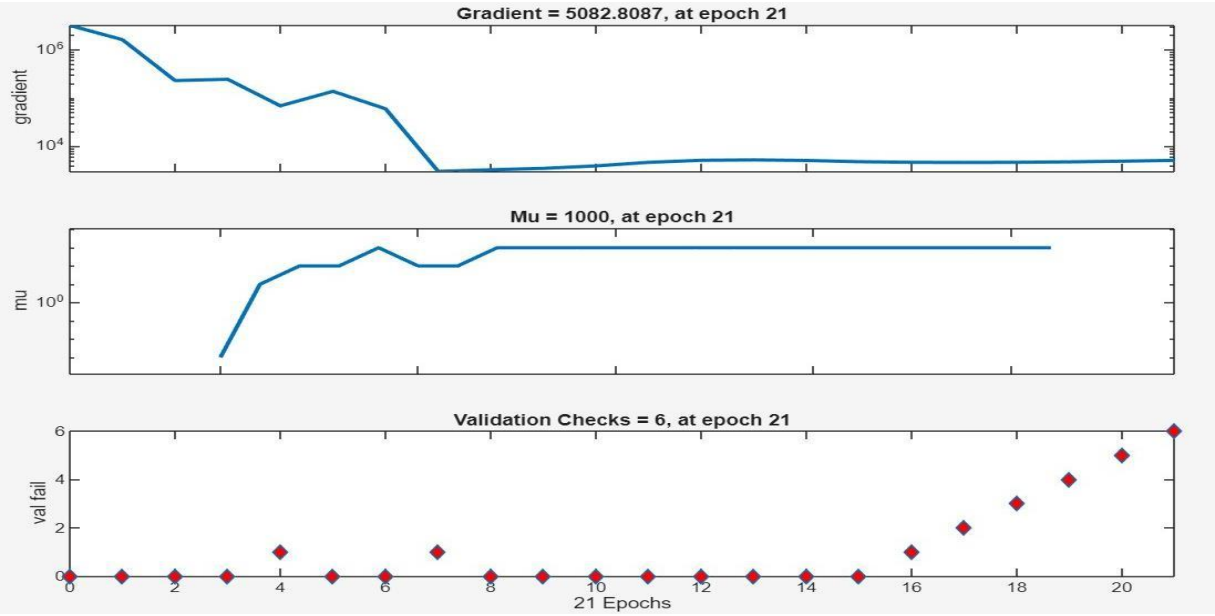


Figure 7.11: Details of Training state plot

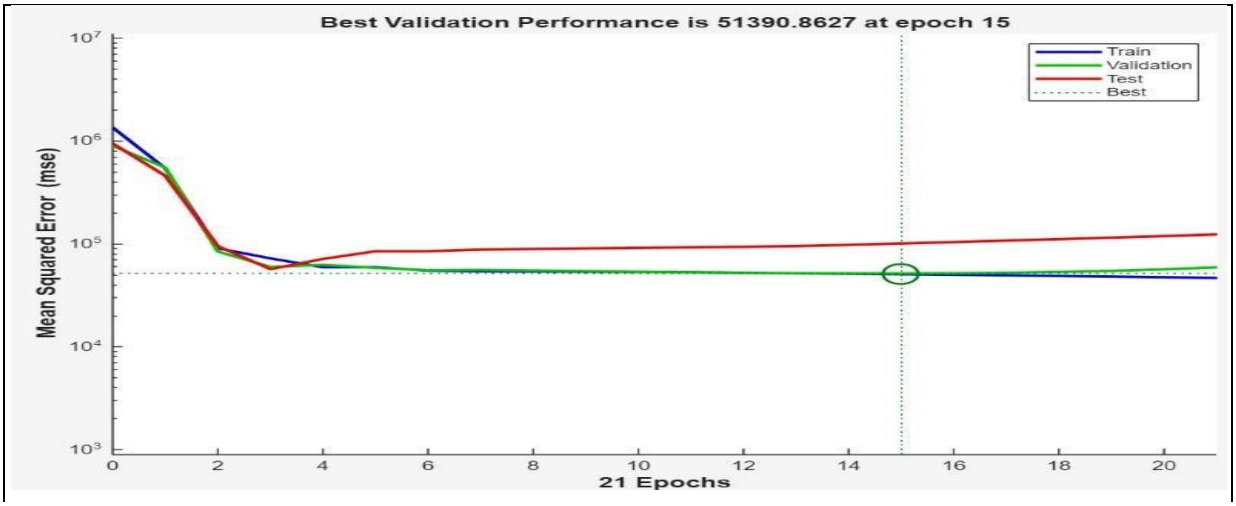


Figure 7.12: Details of Performance plot

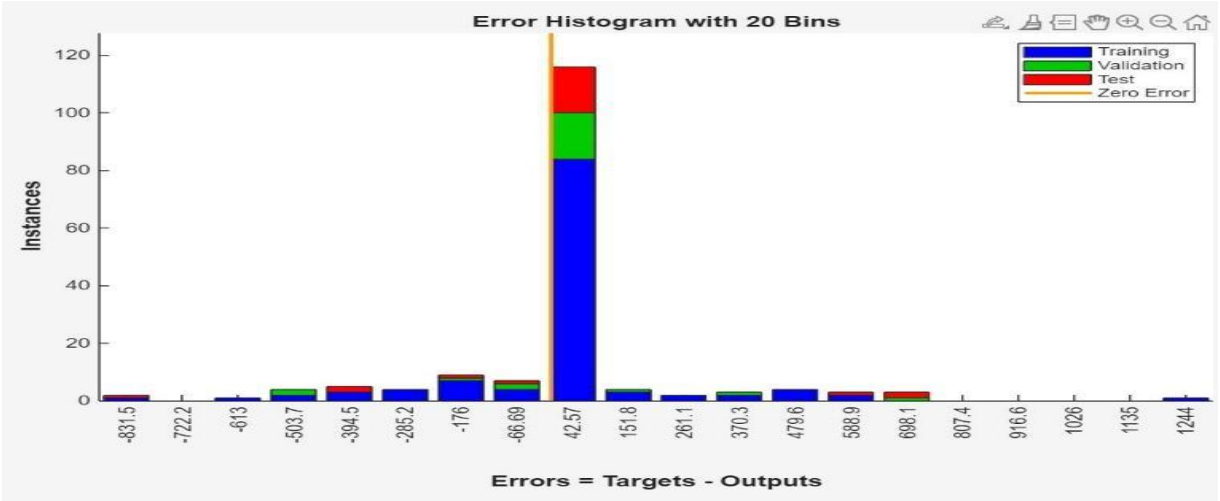


Figure 7.13: Details of Error Histogram plot

IJARCCE ISSN (O) 2278-1021, ISSN (P) 2319-5940

International Journal of Advanced Research in Computer and Communication Engineering

Impact Factor 8.471 ⁜ Peer-reviewed & Refereed journal ⁜ Vol. 14, Issue 5, May 2025

DOI: 10.17148/IJARCCE.2025.145122

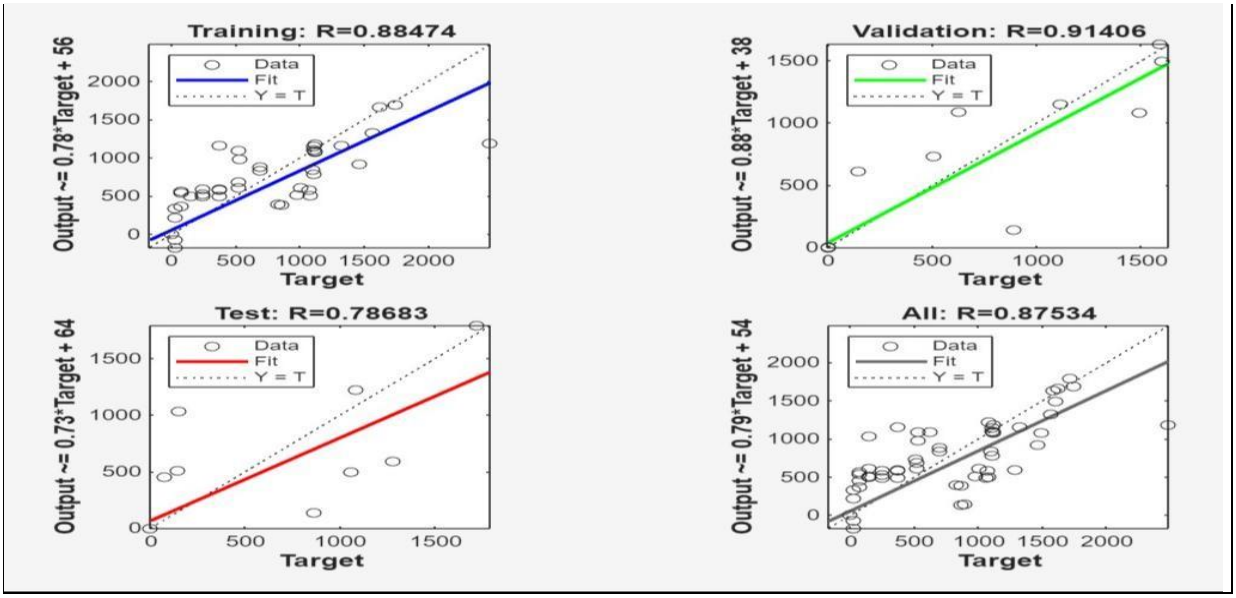


Figure 7.14: Details of Regression plot

## I. 7.2 SOURCE CODE (FROM MATLAB V2024A, MODULE: ANN)

```
function [y1] = myNeuralNetworkFunction(x1)
%MYNEURALNETWORKFUNCTION neural network simulation function.
%
% Auto-generated by MATLAB, 07-Apr-2025 11:22:12.
%
% [y1] = myNeuralNetworkFunction(x1) takes these arguments:
%   x = Qx9 matrix, input #1
% and returns:
%   y = Qx3 matrix, output #1
% where Q is the number of samples.
%#ok<*RPMT0>
% ===== NEURAL NETWORK CONSTANTS =====
% Input 1
x1_step1.keep = [1 2 3 4 5 6 8 9];
x1_step2.xoffset = [207400;0.29;164600;79382;519.6;837.9;7.457e-06;70];
x1_step2.gain = [0.0001388888888888889;54.7945205479452;5.1948051948052e-
05;0.00030362835888872;0.0018789928598 2713;0.0020831163420477;379290.726341741;0
.00357142857142857];
x1_step2.ymin = -1;
% Layer 1
b1 = [2.0412053139549688474; -0.2289250638755573608; -0.97687632213923136781;
0.83520793051493891213; -0.59934839464145728272; 0.17870063912304010034; -
0.006648018214579 6798757; -2.2160574531713472801; -1.4544052144899062284; -
1.7590711682512947256];
IW1_1 = [-0.48165228782056979107 -0.46879196744328816004 0.30527175360904384993 -
1.2862960791974353825 0.6664508546287243318 0.22987577491575769684
1.1166718566081743624 -0.017711412789539526802;2.1172213244337432236
1.1433636082665481482 1.2633717693328527787 -0.20154641648400742349
0.78364528855661 6193 -0.39406305145958026026 -0.36682259151261692454 -
1.0377539732898988234;0.092287347672370151352 -0.80170423555775864036 -
0.63738923891680943079 0.78681023132970073775 -0.88434204378670877578 -
1.0279018589760895441 -0.38500534176722200908 -0.01426222436871 4509007;-
0.36254693132449133941 -0.092210759908535305795 -0.43293261919675646299 -
1.1535806318214756327 -0.43424707823376318405 0.38872488575582098136 -
0.90185248375956894584 0.90915882631711764095;-0.074257035433323834162 -
0.74025802914313409975 0.53600448420896096291 -0.20601923802526678209 -
```

International Journal of Advanced Research in Computer and Communication Engineering
Impact Factor 8.471 ⁜ Peer-reviewed & Refereed journal ⁜ Vol. 14, Issue 5, May 2025
DOI: 10.17148/IJARCCE.2025.145122

```
0.77358500305430855093 0.8299619674539366887 0.0048684386148264910399
2.3552667878391999601;0.84393219259521856657 0.86195746082689717049
0.16756140178933243146 0.21592137950951195702 0.089002364199754017483 -
0.86255331847576155457 0.82340564875599053796 -
0.91388328776363081385;1.0655941270881019722 -1.0018612334218812698 -
0.33902986000414764289 0.73304825217700120277 -0.041089417533779100389 -
1.1811898114749452837 -0.4492884846976385783396 0.38876999450814264669;-
0.94067819664236274058 0.80299073409340537832 0.73191804095544810149
0.13195416209148039255 -0.46646005771781590132 0.63656813102463438714 -
0.84744641285026001132 -2.8266728747779539255;0.13306836630104171282 -
0.20935571225587878974 1.0032434711329090149 -0.94731162197002205527
0.40178670056413989808 -0.24121056895245387985 0.98998873241162488323
0.13875072701487844995;0.13618751578376500633 -0.79796368604783707301 -
0.73613500433561618319 1.0873232606794263067 0.54207163834050164919
0.83532249023909699304 -0.59044765787523478817 -0.81286891981422926268];
% Layer 2
b2 = [0.47475428053863677748; 0.89383198643441841291; -0.82960827788093349788];
LW2_1 = [-0.45022337021532837786 -0.0046777386626125757804
0.44649062972765529711 0.10057976805617939442 0.61686436431957547555 -
0.57191657208299362392 -0.97229536598786281409 -0.50164063888124532653
0.66152154821583675215 -0.23919305918712108205; -0.98797807691682537623
0.07568572897235241459 0.33617188672337705579 0.91974998303486954487
0.96906471351055722963 -0.93073970824803597957 -0.052578526121875537869 -
0.22715437958339199098 0.64929365314014286792 0.85173693717976872719;-
0.13025603929287654648 -0.36170060616903171313 -0.23658817126591971669 -
1.0080260763084918363 0.75019322438115310092 0.59500209942920978534 -
0.43672898091726752856 -1.4535478963979320266 0.15972675852792028728
0.87874527330932128422];
% Output 1
y1_step1.ymin = -1;
y1_step1.gain = [2.64535568129813;242.79387770958;0.000813509794454548];
y1_step1.xoffset = [0.027378;0.00012606;24.817];
% ===== SIMULATION ========
% Dimensions
Q = size(x1,1); % samples
% Input 1 x1 = x1';
xp1 = removeconstantrows_apply(x1,x1_step1); xp1 = mapminmax_apply(xp1,x1_step2);
% Layer 1
a1 = tansig_apply(repmat(b1,1,Q) + IW1_1*xp1);
% Layer 2
a2 = repmat(b2,1,Q) + LW2_1*a1;
% Output 1
y1 = mapminmax_reverse(a2,y1_step1); y1 = y1';
end
% ===== MODULE FUNCTIONS ========
% Map Minimum and Maximum Input Processing Function function y = mapminmax_apply(x,settings)
y = bsxfun(@minus,x,settings.xoffset); y = bsxfun(@times,y,settings.gain);
y = bsxfun(@plus,y,settings.ymin); end
% Remove Constants Input Processing Function function y = removeconstantrows_apply(x,settings) y =
x(settings.keep,:);
end
% Sigmoid Symmetric Transfer Function function a = tansig_apply(n,~)
a = 2 ./ (1 + exp(-2*n)) - 1; end
% Map Minimum and Maximum Output Reverse-Processing Function function x =
mapminmax_reverse(y,settings)
```

International Journal of Advanced Research in Computer and Communication Engineering

Impact Factor 8.471 ⁜ Peer-reviewed & Refereed journal ⁜ Vol. 14, Issue 5, May 2025

DOI: 10.17148/IJARCCE.2025.145122

```
x = bsxfun(@minus,y,settings.ymin); x = bsxfun(@rdivide,x,settings.gain); x = bsxfun(@plus,x,settings.xoffset);
end
```

## VIII. DISCUSSION

Research on railway wagon wheels aims to improve wheel-rail contact, minimize the noise and wear, increase safety, and maximize the performance, including investigating novel materials and designs. Both the original profile and the modified wheel-in have undergone examination, where the material in the inner structure optimized. Additionally, these two studies' outcomes are contrasted. Plotting of displacements and stresses against the wheel is done, and observed that,

- When the load changes, there is very tiny variation in strain, stress, and total deformation.
- There is very small variation in total deformation, strain, and stress, as the applied force varies.
- The natural frequency variations in modal analysis result in very slight variations in total deformation, strain, and stress.

## IX. CONCLUSION

In this practice, 3D Rail-Wheel (R/W) contact static analysis, fatigue, elastic strain, and equivalent von-mises stresses are analysed using MATLAB. To guarantee accurate findings, boundary conditions and realistic-FE loading are applied. The total deformation, equivalent strain, equivalent stress (von mises), and level all affect how long tiredness lasts.

MATLAB enhances earlier techniques for simulating, modelling, and evaluating rail-wheel contact mechanics. Sometimes, traditional methods and computer approaches yield static results without considering the full rolling motion of the wheel. MATALB is used to calculate stress, employing a sub-modelling technique for increased speed and precision. The fatigue life is calculated using the stress history.

A critical plane method for multi-axial fatigue life prediction is presented in this paper. Unlike earlier models that just considered stress, the current critical plane model takes material properties and stress into account. The fatigue start life of wheel/rail contact issues are predicted using the new multi-axial fatigue model, and after the analysis the following conclusions are derived.

- ❖ The stresses on the roadwheel assembly are investigated in this study. Contact sites were shown to have greater levels of stress. Additionally, the rail will encounter the highest stresses while in operation.
- ❖ We made design and material improvements to the models. This study demonstrated that design and material optimization may be accomplished with little extra requirements.
- ❖ To change the material and reduce weight, we improved the rail wheel design. In railway weight optimization, various alloy steel and carbon steel grades are assessed using the same boundary conditions.
- ❖ For alloys, the railway wheel's weight is reduced by around 3%.

## REFERENCES

[1]. Prof. Chetan Patil, Tejas Nandani, Hate Nagaraj Gouda, Shashank D. Vighneshi, Meghana Chittapur. “Enhancement of Railway Safety Measures through Deep Learning Algorithm to Identify Railway Wheel Defects,” International Journal of Research Publication and Reviews, Volume 5, May 2024, pp 10154-10161.

[2]. Muhammad Zakir Shaikh, Mariofanna Milanova, Zeeshan Ahmed, Enrique Nava Baro, Samreen Hussain, “Deep learning-based identification and tracking of railway bogie parts,” Alexandria Engineering Journal 107, (2024), pp.533–546.

[3]. Sumit Kumar Das, “Wheel Defect Detection with Advanced Machine Learning,” International Journal for Research in Applied Science & Engineering Technology (IJRASET), Volume 11, Issue II, Feb 2023, pp.500-504.

[4]. Suhansa Rodchua, Rommel Jefrin, “Application of Robotics in Manufacturing Industry IndM 5230: Seminar in Industrial Management”.

[5]. Zongyi Xing, Zhenyu Zhang, Xiaowen Yao, Yong Qin, Limin Jia, “Rail wheel tread defect detection using improved YOLOv3”, Journal of the International Measurement Confederation (IMEKO), Volume 203, 15 November 2022, 111959.

[6]. Alexandre Trilla, Alstom, John Bob-Manuel, Benjamin Lamoureux, Xavier Vilasis-Cardona " Integrated Multiple-Defect Detection and Evaluation of Rail Wheel Tread Images using Convolutional Neural Networks", International Journal of Prognostics and Health Management, May 2021, pages.1-19.

International Journal of Advanced Research in Computer and Communication Engineering

Impact Factor 8.471 ⁜ Peer-reviewed & Refereed journal ⁜ Vol. 14, Issue 5, May 2025

DOI: 10.17148/IJARCCE.2025.145122

[7]. Shivendra Nandan, Rishikesh Trivedi, Satyajeet Kant, Javed Ahmad, M. Maniraj, "Design, Analysis and Prototype Development of Railway Wagons on Different Loading Conditions," international Journal of Engineering Applied Sciences and Technology, Volume 4, Issue 10 February 2020, Pages 122-129.

[8]. Basavaraj, Dr. Sridhar.B. S, "Optimization of Design Parameters, Performance Analysis of Rail-Wheel Assembly," International Journal of Engineering Research & Technology (IJERT), Volume 8, Issue 14/Special Issue – 2020, pp.14-19.

[9]. Madalina Ciotlaus, Gavril Kollo, Vladimir Marusceac, Zsolt Laszlo Orban. "Rail wheel Interaction and Its Influence on Rail and Wheels Wear," Hindawi Mathematical Problems in Engineering, Volume 2020, Article ID 9579510, 10 pages. 56

[10]. B. Jagadeep, P. Kiran Kumar, K. Venkata Subbaiah, "Stress analysis on rail wheel contact," International Journal of Research in Engineering, Science and Management (IJERT), Volume-1, Issue-5, May 2018, pp.47-52.

[11]. L. Venugopal, M. Sunil Kumar, "Optimum design and performance analysis on a rail wheel assembly of rail mounted storage cum resting fixture," ISSN 2319 8885, Volume 06, Issue.04, february-2017, pp.0699-0705.

[12]. B. Vinod Kumar, M. Suneetha, Dr.N. Venkatachalapathi. "Modeling and Analysis of Railway Wagon, International journal & magazine of engineering," technology management and research (IJERT), Volume. 4, Issue 11, January 2017, pp.403 407

[13]. Prof. Shaikh S.M., Mahesh Buddhe. "Analysis Of Rail-Wheel Contact Stresses Using Finite Element Method in Comparison with Analytical Solution," International Journal of Innovations in Engineering Research and Technology [IJIERT], Volume 3, Issue 8, Aug-2016, pp.31 -37.

[14]. Prachi Katheriya, Veerendra Kumar, Anshul Choudhary, Raji Nareliya. "An investigation of effects of axle load and train speed at rail joint using finite element method," International journal of research in engineering and technology (IJRET), Volume: 03, Issue: 08, Aug-2014, pp. 41- 47.

[15]. P. Vinod, U. Koteswara Rao, Ch. Kishore Reddy, "Analysis of Railway Wheel to Study the Stress Variations," International Journal of Engineering Research & Technology (IJERT), Volume 03, Issue 02, February 2014, pp. 1286-1291.